

Shear behaviour of steel-fibre-reinforced concrete simply supported beams

1 Ali A. Abbas PhD, DIC, FHEA

Senior Lecturer in Structural Engineering, School of Architecture, Computing and Engineering, University of East London, London, UK

2 Sharifah M. Syed Mohsin PhD, DIC

Senior Lecturer, Faculty of Civil and Earth Resources, University of Malaysia Pahang, Kuantang, Malaysia

3 Demetrios M. Cotsovos Dipl Ing, MSc, PhD, DIC, CEng

Lecturer in Structural Engineering, Institute of Infrastructure and Environment, School of the Built Environment, Heriot-Watt University, Edinburgh, UK

4 Ana M. Ruiz-Teran PhD, CEng MICE, FHEA

Lecturer in Bridge Engineering, Department of Civil and Environmental Engineering, Imperial College London, London, UK



The structural behaviour of steel-fibre-reinforced concrete beams was studied using non-linear finite-element analysis and existing experimental data. The work aim was to examine the potential of using steel fibres to reduce the amount of conventional transverse steel reinforcement without compromising ductility and strength requirements set out in design codes. To achieve this, the spacing between shear links was increased while steel fibres were added as a substitute. Parametric studies were subsequently carried out and comparisons were also made with BS EN 1992-1-1 predictions. It was concluded that the addition of steel fibres enhanced the load-carrying capacity and also altered the failure mode from a brittle shear mode to a flexural ductile one. The provision of fibres also improved ductility. However, interestingly it was found that adding excessive amounts of fibres led to a less-ductile response. Overall, the study confirmed the potential for fibres to compensate for a reduction in conventional shear reinforcement.

Notation

a	shear span
d	effective depth
E_a	energy absorption
$E_{a,0}$	energy absorption of the control specimen
M_{rd}	bending moment capacity
P	lateral monotonic load
P_{BMC}	load calculated based on bending moment capacity
P_{max}	load-carrying capacity
$P_{max,EXP}$	load-carrying capacity based on experimental data
$P_{max,DES}$	load-carrying capacity based on current design guidelines
$P_{max,FEA}$	load-carrying capacity based on finite-element analysis
$P_{max,0}$	load-carrying capacity of the control specimen
P_{sc}	load calculated based on shear capacity
P_u	ultimate load
P_y	load at yield
$P_{y,0}$	load at yield of the control specimen
SI	stirrup spacing increased
V_f	volume fraction of the fibres
V_{rd}	shear capacity

δ_y	deflection at yield
δ_u	ultimate deflection
μ	ductility ratio
$\mu_{,0}$	ductility ratio of the control specimen

1. Introduction

Concrete has become one of the most important construction materials widely used in many types of engineering structures. As plain concrete is a brittle material, several attempts have been made to improve its ductility and one of these means is by adding fibres to the concrete mix. The work presented in the present paper aims to examine the structural response – particularly the shear behaviour – of steel-fibre-reinforced concrete (SFRC) beams using non-linear finite-element analysis (NLFEA). The effect of the steel fibres is directly modelled into the existing concrete material model employed by the commercial software package Abaqus (2007) to describe its non-linear behaviour. This is achieved by appropriately modifying the stress–strain relationship of concrete in uniaxial tension. The resulting model was calibrated using existing experimental data (Campioni *et al.*, 2006) on the shear response of SFRC beams with fibre volume fraction (V_f) of 1%. The beams were initially designed with shear reinforcement less than that required

in order to induce shear failure (so in one arrangement some shear links were provided, whereas no links were provided in the other cases). Subsequently, parametric studies were carried out using NLFEA to examine SFRC beams with increased spacing between shear links (including their complete removal), but with the full practical range of fibre dosages considered. Conclusions were thus made on the potential for fibres to compensate for reduction in conventional shear reinforcement.

2. Constitutive models for SFRC and modelling strategy

2.1 Cracking process and the role of fibres

The failure of plain concrete is governed by the formation of a single crack. Before the initiation of the first crack, the material exhibits linear elastic behaviour. A crack forms when the maximum principal tensile stress exceeds the tensile strength of concrete, thus resulting in localised material failure. The plane of the crack is normal to the direction in which the largest principal tensile stress acts. These fracture processes create voids within the material (i.e. macro-cracks), which continue to extend as the load is increased. By contrast, in SFRC, upon crack formation the crack opening is restrained by the fibres. The latter provides a crack arresting/bridging effect to resist further crack opening. There are different potential failure modes depending on the effectiveness of the fibres in providing crack bridging. Therefore, fibres can be effective in enhancing both the bending and shear capacity of concrete sections as they control the crack propagation under both flexural and shear-induced diagonal tension.

2.2 Tensile behaviour

The structural response of SFRC elements is characterised by its tensile post-cracking behaviour. A number of available constitutive models for SFRC have been identified such as those proposed by Barros and Figueiras (1999, 2001), Lok and Pei (1996), Lok and Xiao (1999), Rilem Technical Committees (2000, 2003) and Tlemat *et al.* (2006). The constitutive relations have been developed to describe the uniaxial tensile stress–strain relationship of SFRC. In particular, they depict the effect of fibres on changing the post-cracking behaviour of concrete from the brittle sharp drop associated with plain concrete to either tension softening or hardening response, depending on the fibre amount provided, fibre geometry and shape and bond stress. In these models, the residual strength beyond the cracking point of concrete is made up of two components: the steel fibres bridging the crack and the concrete matrix followed by the pull-out phase (i.e. bond failure). The main characteristics of the models were closely studied and a calibration study was undertaken by Abbas *et al.* (2010a, 2010b) and Syed Mohsin (2012) using NLFEA to examine these models and compare their predictions with existing experimental data on numerous SFRC beam samples. Consequently, it was found that the use of the model proposed by Lok and Xiao (1999) resulted in predictions that were in best agreement with the experimental data. Even in instances where there was a slight difference, the discrepancy was always on the safe side (in design terms), with

the model predictions not overestimating actual strength results. Unlike many other SFRC models, the Lok and Xiao (1999) model is applicable for a reasonably wide practical range of fibre volume fractions (i.e. 0.5% to 3.0%), which covers the range investigated in the present research work. The model is also versatile as it allows for definition of different values of aspect ratio (L/d) and bond stress (τ_d) as well as taking into account the effect of the randomness in the distribution of fibres. Therefore, it was selected for the subsequent parametric studies.

2.3 Compressive behaviour

Published work on SFRC (e.g. Lok and Xiao, 1999; Rilem Technical Committees, 2000, 2003; Tlemat *et al.*, 2006) suggests that the compressive behaviour of SFRC can be conveniently assumed to be similar to that of plain concrete. Investigations carried out by Bencardino *et al.* (2008) support this conclusion as the observed results show that the addition of steel fibres does not significantly affect the compressive strength of concrete (with potential improved ultimate strain safely ignored). Therefore, in the present work, the steel fibres are considered to have no effect on the compressive behaviour of plain concrete.

2.4 Shear behaviour

The amount of crack opening affects the shear behaviour. Usually in the NLFEA of reinforced-concrete (RC) structures, ‘shear retention’ is used to allow for the effect of aggregate interlock and dowel action. Fibres provide a similar effect on shear response (i.e. in a direction parallel to the crack) and, therefore, it was modelled using the ‘shear retention’ part of the Abaqus (2007) concrete model. The shear stiffness of the concrete decreases when crack is propagated. Therefore, in order to allow for degradation in shear stiffness owing to crack propagation, the shear modulus was reduced in a linear fashion from full shear retention (i.e. no degradation) at the cracking strain by 50% at the ultimate tensile strain. This is an average value which is judged to be representative of the effect of aggregate interlock, dowel action and the contribution of fibres parallel to the crack plane. Moreover, the shear resisted is attributable to diagonal-tension stresses rather than direct shear. Therefore the main contribution of fibres will be through tensile resistance (perpendicular to the crack plane), which is represented fully through the constitutive model adopted, while a reasonable estimation of the shear retention value will suffice.

2.5 Conventional steel main bars and stirrups

In the present study, the steel properties for longitudinal bars and shear links were modelled using a standard elastic-plastic material model. The stress–strain relation adopted is the one recommended in BS EN 1992-1-1 (BSI, 2004), which employs isotropic hardening in which the yield stress increases as plastic straining occurs. An ultimate tensile strain was also defined to detect any failure on the steel main bars or stirrups. The constitutive model adopted is representative of the behaviour of the corresponding bars used in the experiments and the key values such as the yield stress were replicated in the numerical work.

2.6 NLFEA strategy

A brief summary of the NLFEA strategy adopted is provided here, whereas a detailed background on the finite-element method can be found elsewhere (Zienkiewicz and Taylor, 2005). Abaqus (2007) offers few material models for non-linear analysis of plain concrete and associated cracking processes. The models also allow for the effect of tension stiffening to be included (this effect is related to the stiffness provided by concrete between cracks or interaction between concrete and reinforcement). This is achieved effectively by modifying the post-cracking tensile stress–strain diagram. Therefore, this was conveniently used to input the tensile constitutive models for SFRC.

The Abaqus material model adopted for the present study to describe concrete behaviour is the ‘brittle cracking model’. This model is designed for cases in which the material behaviour is dominated by tensile cracking, as is normally the case for structural concrete. As the model focuses on the all-important brittle tensile aspect of concrete behaviour, a simplification has been introduced by assuming compressive behaviour to be linear elastic. The behaviour of concrete in tension (prior to cracking) is assumed to be linear elastic. The post-cracking phase is described using tension-stiffening, which allows the uniaxial stress–strain relation to be defined. This is justified, particularly for three-dimensional (3D) modelling, as at least one of the three principal stresses needs to be tensile and exceeding the tensile strength to initiate cracking (whereas the other two principal stresses could be compressive). The main attractive feature of the model is that it focuses on the main mechanisms for failure in concrete, namely its brittleness and cracking (predominantly in tension). Thus the simplification made with regard to compressive behaviour is intended to make the solution efficient without affecting its accuracy of mimicking real behaviour of concrete. A smeared crack approach is adopted to model the cracking process that concrete undergoes. For purposes of crack detection, a simple Rankine criterion is used to detect crack initiation (i.e. a crack forms when the maximum principal tensile stress exceeds the specified tensile strength of concrete).

In the present study, the concrete medium was modelled by using a mesh of 3D brick elements. The mesh adopted has an element size of 20 mm, which was determined based on a sensitivity analysis carried out in order to assess the effect of the mesh size on the accuracy of the numerical predictions. Thus, the calibration work carried out against experimental data was crucial in selecting the best mesh size that accurately represents the true structural response (i.e. the mesh which best replicates experimental results). One-dimensional (1D) bar elements representing conventional steel reinforcement bars and shear links were placed to mimic the actual arrangement in the specimens modelled (e.g. cover allowed for). In order to make the numerical solution efficient and to enhance numerical stability (which is adversely affected by cracking), the analysis was carried out using the dynamic solver as a quasi-static one (i.e. at a low rate of loading). This was used in conjunction with the explicit dynamic procedure

available in Abaqus/Explicit (Abaqus, 2007). The ratio between kinetic and strain energies was checked to ensure that it remains below $\sim 5\%$, indicating that the analysis remains quasi-static. In addition, the load was applied using a displacement based method to minimise convergence problems.

Generally, the analysis will automatically terminate once the model analysed fails. Nevertheless, it is important to observe the results obtained and make a judgement of acceptable results to be used prior to failure. Also in some cases the programme does not terminate by itself, which is similar to the situation with experimental work where some judgement needs to be applied regarding the failure point in order to stop the experiment. Therefore, in the present study, failure was considered to occur once a sudden high jump in the kinetic energy was identified. This high kinetic energy is deemed to be the result of excessive movement of the structure, indicating extensive cracking and deformation associated with structural failure. A similar approach is commonly used in the modelling of RC structures (e.g. Zheng *et al.*, 2012). This was also confirmed by examining both the deformed shape and cracking pattern of the structure.

3. Calibration with experimental work

A series of SFRC simply supported beams with and without stirrups were tested under monotonic loading by Campione *et al.* (2006) to study their shear behaviour. Steel fibres were added to investigate whether or not fibres can partially or fully substitute transverse stirrups and retain the same level of shear resistance. Initially, two sets of experimental data (Bresler and Scordelis, 1963) and (Hughes and Spiers, 1982) for conventionally reinforced concrete beams (i.e. without fibres) were modelled using Abaqus. The beams were chosen to include both ductile and brittle modes of failure to ensure that the proposed finite-element analysis (FEA) predictions are reliable. The calibration of these two particular tests was useful in examining the accuracy of the FEA results in the absence of fibres. This is a crucial step so that any differences between the predictions of analyses using specimens with and without fibres can be reasonably interpreted to indicate change in structural response rather than a modelling discrepancy. The results show that the FE model is capable of yielding results that are in good agreement with experimental data for RC structures. Once this was confirmed (Syed Mohsin, 2012), comparisons with experimental data on SFRC beams were carried out as discussed next.

3.1 Experimental cases considered

Two SFRC beams tested by Campione *et al.* (2006) were selected to be calibrated and then adopted for the ensuing parametric studies on simply supported beams. The beams’ dimensions and reinforcement and loading arrangements are shown in Figure 1(a). One of the beams was reinforced with shear links, whereas the other had no links. The concrete cylinder compressive strength was 41.2 MPa, while the tensile strength was assumed to be 9% (i.e. 3.7 MPa) of the compressive strength for modelling purposes. The tensile strength estimate is similar to the value

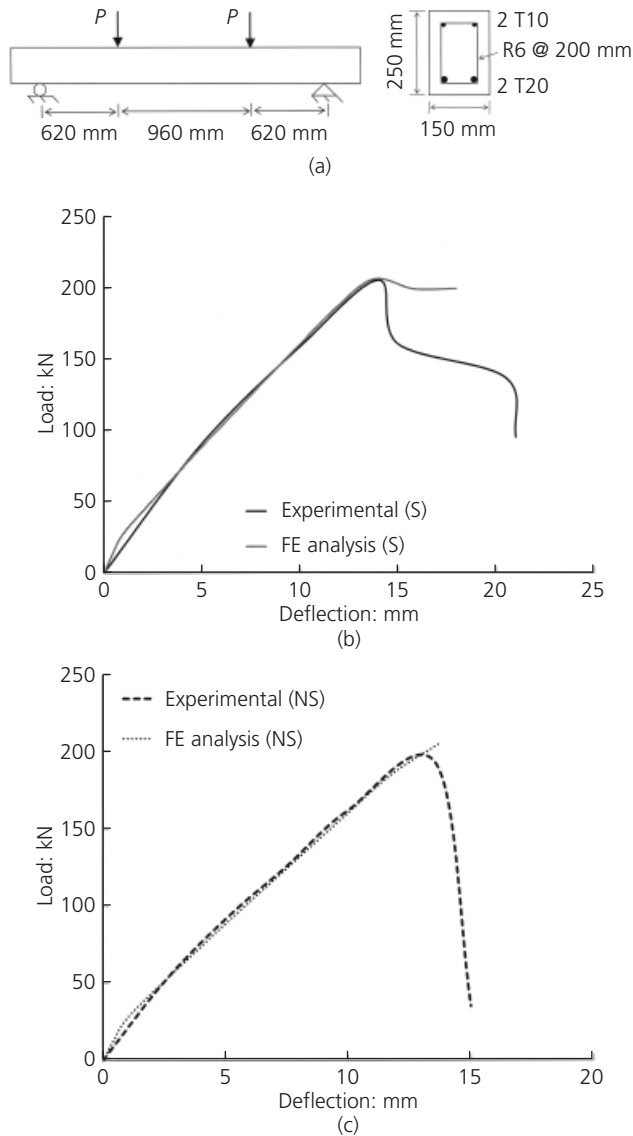


Figure 1. Calibration results for SFRC beams tested by Campione *et al.* (2006): (a) loading arrangement and reinforcement detailing; (b) results for beams with stirrups (i.e. S) and (c) without stirrups (i.e. NS)

recommended in BS EN 1992-1-1 (BSI, 2004). The yield stresses of main bars and stirrups were 610 MPa and 510 MPa, respectively. Steel fibres used were hooked-end with 30 mm length and 0.5 mm diameter added at a volume fraction of $V_f = 1\%$. The beams selected for calibration work had a shear span (a) to effective depth (d) ratio of $a/d = 2.8$. Taking advantage of the symmetrical conditions at the mid-span of the beam, only half of the beam was modelled. Elastic steel plates with 20 mm thickness were added at the support and loading regions to mimic the experimental set-up and help avoid development of stress concentrations leading to premature localised failure in the FE simulation.

3.2 Results of calibration work

A comparison between the experimental and numerical results is presented in Figures 1(b) and 1(c) for both beams with and without stirrups (denoted by symbols S and NS, respectively). The two sets of results show that there is good agreement between the experimental and numerical results, with the load–deflection curves almost identical, confirming the reliability and accuracy of the latter. FEA-based kinetic energy results are depicted in Figure 2 and a sudden large increase in energy was taken to indicate failure (i.e. the presence of large/extensive cracks that impair structural integrity).

3.3 Additional samples of calibration work

As mentioned earlier, an extensive range of calibration studies was carried out at both the material and structural levels at the initial phase of the present investigation. Full details of these calibrations are available elsewhere (Syed Mohsin, 2012). The details of the case study adopted for the present paper were discussed in the preceding Section 3.2. Nevertheless, two further case studies are presented in Figures 3 and 4, which demonstrate the accuracy of the FE model predictions compared to existing experimental data on beams that failed in bending and shear modes, respectively. Figure 3(a) depicts the arrangement of the SFRC simply supported beam tested by Cho and Kim (2003), while the corresponding calibration results are presented in Figure 3(b). The concrete cylinder compressive strength was 25.3 MPa, the yield and ultimate strengths were 400 MPa and 600 MPa, respectively, for both longitudinal and transverse reinforcement bars used. Steel fibres adopted were hooked-end with 36 mm length and 0.6 mm diameter added at a volume fraction of $V_f = 1\%$. Figure 4(a) shows the arrangement of the SFRC beam tested by Sharma (1986) with the results of the comparison between the test results and corresponding numerical predictions depicted in Figure 4(b). Steel fibres used have a length of 50 mm, a diameter of 0.6 mm and a volume fibre ratio of 0.96%. The

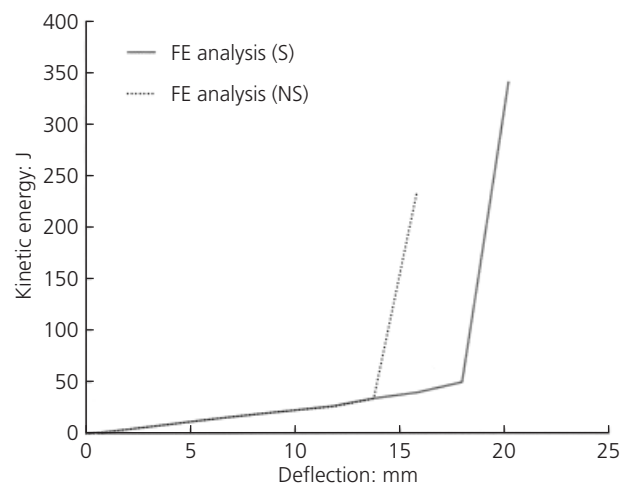


Figure 2. Kinetic energy plots to determine failure for calibration work of SFRC simply supported beams

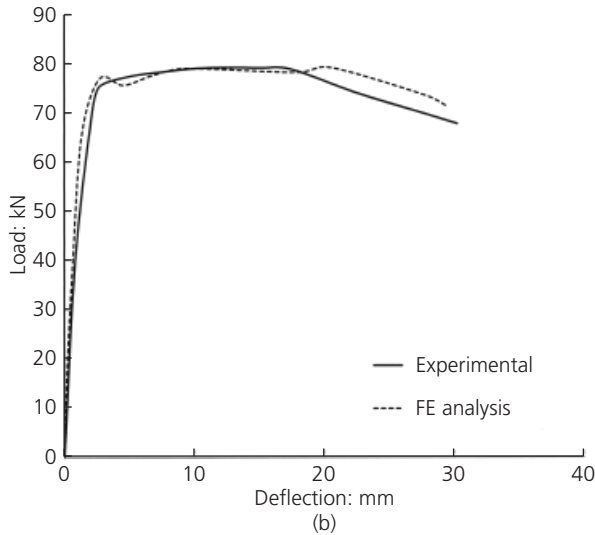
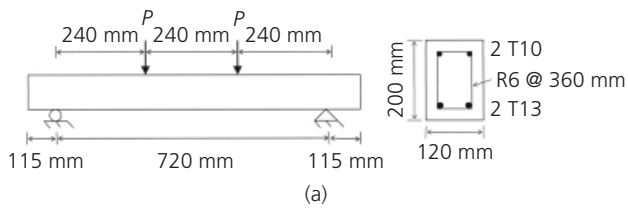


Figure 3. Comparison between numerical and experimental results for SFRC beam tested by Cho and Kim (2003): (a) dimensions and loading arrangement and (b) results

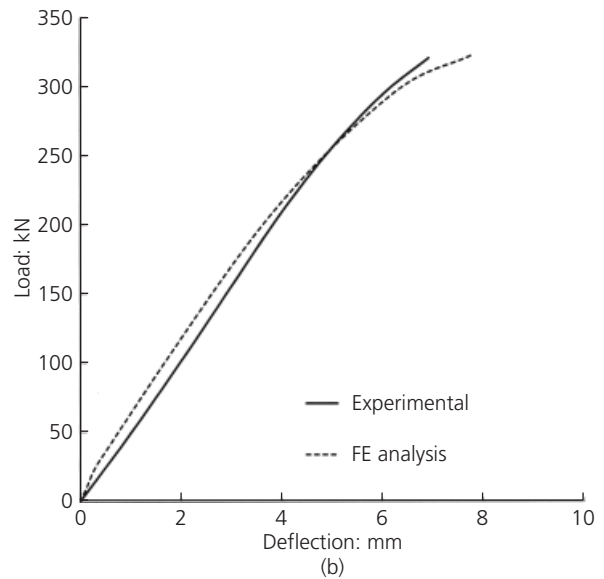
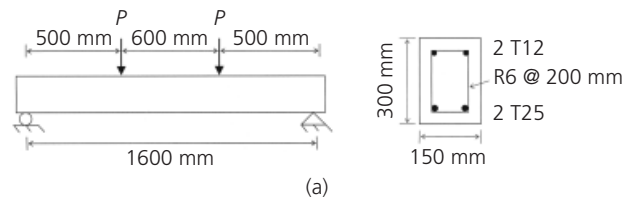


Figure 4. Comparison between numerical and experimental results for SFRC beam tested by Sharma (1986): (a) dimensions and loading arrangement and (b) results

concrete compressive strength was 47.7 MPa and the yield and ultimate strengths (of both longitudinal and transverse reinforcement bars) were 400 MPa and 460 MPa, respectively. The results of Figures 3(b) and 4(b) show that the FE-based results agree well with their experimental counterparts and mimic both the ductile and brittle responses reasonably accurately, thus confirming the reliability of the FE model adopted.

4. Parametric studies on simply supported SFRC beams

Following the calibration work, parametric studies were carried out incorporating two key parameters: the increase in spacing between shear stirrups (SI) and steel fibres volume fraction (V_f). The beams were modelled with reduced stirrups in order to induce a shear mode of failure, whereas fibres were added to examine whether or not they can compensate for the loss in conventional shear reinforcement. Therefore, beams were considered with $SI = 0\%$, 50%, 100% and with no stirrups (NS). The calibrated spacing of 200 mm was adopted as $SI = 50\%$ so that spacing changes can be applied either side of this value. Thus, $SI = 0\%$, 50% and 100% correspond to 135 mm, 200 mm and 270 mm, respectively. This was coupled with fibres provided at $V_f = 0\%$, 1%, 1.5%, 2% and 2.5%. The tensile stress-strain diagram adopted for the SFRC beams is shown in Figure 5 with the key points on the curves summarised in Tables 1 and 2.

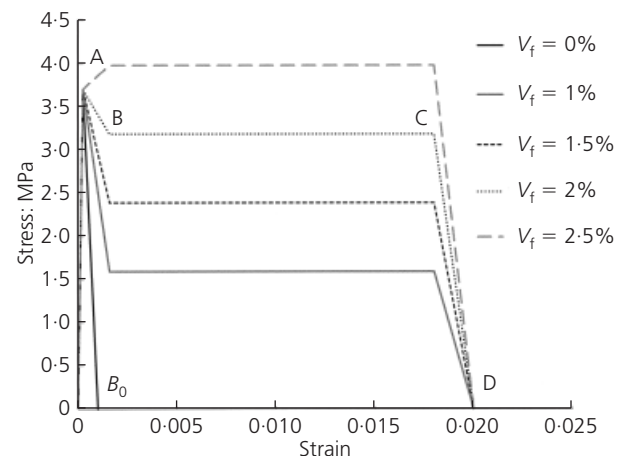


Figure 5. Stress-strain relations in tension adopted for parametric studies of SFRC simply supported beams

4.1 Load-deflection curves

The load-deflection curves for simply supported beams with increases in stirrup spacing of $SI = 0\%$, 50%, 100% and no stirrup (NS) are presented in Figures 6(a) to (d), respectively. In

Point	Strain: ‰	Stress (MPa) for $V_f = 0.0\%$
Origin	0	0
Peak tensile stress (A)	0.247	3.70
Ultimate tensile strain (B_0)	1.0	0

Table 1. Tensile stress–strain parameters adopted for plain concrete

In addition, a summary of the key load values and their respective deflections is provided in Tables 3–6, in which P_y represents the load at yield, P_{max} the maximum load (i.e. strength), P_u the ultimate load (i.e. residual strength), δ_y the deflection at yield, δ_u the ultimate deflection and μ the ductility (defined as $\mu = \delta_u/\delta_y$). The load–deflection curves show that the beam without fibres failed early confirming a brittle mode of failure associated with shear strength deficiency. In contrast, there is a gradual increase in strength and ductility as the fibre content is increased. The stiffness has also increased noticeably in comparison to the case without fibres, indicating that SFRC beams deflect less than their counterparts without fibres. This suggests that there are clear benefits of adding fibres at both the serviceability and ultimate limit states, which are important design considerations.

4.2 Strength

The load–deflection curves show that the load-carrying capacity of the beams increased as more fibres were added. The beam without fibres and $SI = 0\%$ failed at a maximum load (P_{max}) of 197.27 kN and ultimate deflection (δ_u) of 17.97 mm. This beam was considered as the reference beam and was named the control beam specimen (CB) to be compared with the remaining beams in the parametric studies. The increase in P_{max} of the SFRC beams compared to that in the control specimen was up to an average of 16% in all beams with different stirrup arrangements. Furthermore, the load at yield (P_y) increased by up to 15% higher than that in the control beam. The enhancement to shear strength owing to fibres confirms their potential to substitute for a reduction in conven-

tional transverse reinforcement. The steel fibres extend across diagonal shear cracks (induced by tensile principal stresses) and contribute to shear capacity by resisting these diagonal tension stresses.

4.3 Ductility

The ductility of the beams can be determined from the ultimate deflection at failure (δ_u). The latter is associated with the ultimate load, which was taken as the minimum of the load at failure or 85% of the maximum load (i.e. $P_u \geq 0.85P_{max}$). This limit was introduced to ensure the practical usefulness of the ductility enhancement (i.e. to check that the post-peak ‘softening’ trend observed on the load–deflection curves is not significant). The increases of δ_u in the SFRC beams compared to that in the control specimen were up to 63%, 67%, 50% and 12%, for the beams with $SI = 0\%$, 50%, 100% and no stirrups, respectively. The results show that the addition of fibres enhances the ductility of the beams, even in the beams with no stirrups (albeit the enhancement in the latter is considerably less than the case with stirrups, indicating the severity of shear reinforcement reduction when stirrups were completely removed).

4.4 Principal strains and crack patterns

The principal strain contours and vectors at failure were studied and the data provided insight into the failure mechanism as well as cracking formation and patterns.

4.4.1 Principal strain contours

The principal strain contours for the SFRC simply supported beams were analysed. In particular, zones with strains exceeding critical strain values such as 0.001 (i.e. tensile cracking strain) for beams without fibres and 0.02 (i.e. fibre pull-out strain) for SFRC beams were studied. Similarly, areas where the compressive strain was higher than the ultimate strain of concrete (i.e. -0.0035) were also examined. It was found that the fibres led to a reduction in crack formation and propagation. Moreover, pull-out failure of fibres occurred at limited zones. These zones in the SFRC beams were not at the same location; however, they always occurred in a region between the lateral point load (P) and the beam mid-span (see Figure 1(a)). This is because the bending moment is constant along this region and there is no single peak moment to induce a

Point	Strain: ‰	Stress: MPa			
		$V_f = 1.0\%$	$V_f = 1.5\%$	$V_f = 2.0\%$	$V_f = 2.5\%$
Origin	0	0	0	0	0
Peak tensile stress (A)	0.247	3.70	3.70	3.70	3.70
Beginning of plateau (B)	1.59	1.59	2.39	3.18	3.98
End of plateau (C)	18	1.59	2.39	3.18	3.98
Ultimate tensile strain (D)	20	0	0	0	0

Table 2. Tensile stress–strain parameters adopted for SFRC

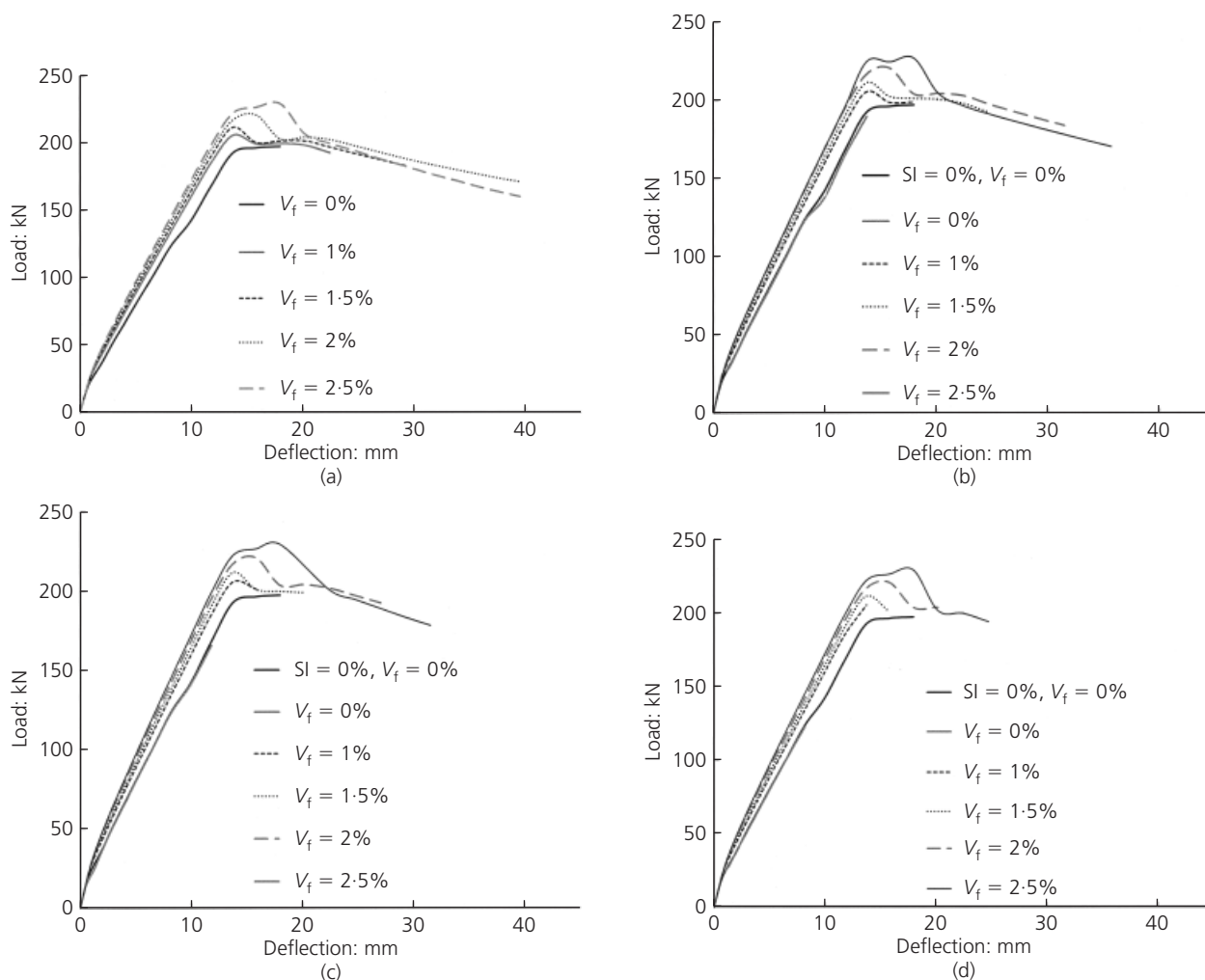


Figure 6. Load–deflection curves for SFRC beams with (a) $SI = 0\%$, (b) $SI = 50\%$, (c) $SI = 100\%$ and (d) no stirrups (NS)

V_f : %	P_y : kN	δ_y : mm	P_u : kN	δ_u : mm	P_{max} : kN	$\frac{P_u}{P_{max}}$: %	$\mu = \frac{\delta_u}{\delta_y}$
0	192.77	13.76	197.27	17.97	197.27	100	1.31
1	205.78	13.76	192.58	22.46	205.76	94	1.63
1.5	211.69	13.76	182.90	29.30	211.69	86	2.13
2	217.12	13.76	187.63	29.00	220.74	85	2.11
2.5	222.26	13.76	194.83	24.50	229.21	85	1.78

Table 3. Results summary for beams with $SI = 0\%$

fixed failure point. More than one small crack formed in this region. Throughout the analysis, only one of these small cracks developed earlier will continue to propagate into a large one. This led to a different location for the main crack at failure (i.e. where fibres were pulled out).

4.4.2 Principal strain vectors

The principal strain vectors for the beams with $SI = 0\%$, 50%, 100% and no stirrups are presented in Figures 7(a) to 7(d), respectively. It is interesting to note that the layout of principal strain vectors (for each different stirrup arrangement, from

V_f : %	P_y : kN	δ_y : mm	P_u : kN	δ_u : mm	P_{max} : kN	$\frac{P_u}{P_{max}}$: %	$\mu = \frac{\delta_u}{\delta_y}$
0 (CB)	192.77	13.76	197.27	17.97	197.27	100	1.31
0	189.94	13.76	189.94	13.76	189.94	100	1.00
1	205.77	13.76	199.14	17.97	205.77	97	1.31
1.5	211.59	13.76	192.36	24.73	211.59	91	1.80
2	217.03	13.76	187.62	30.00	220.73	85	2.18
2.5	222.23	13.76	193.15	25.30	227.23	85	1.84

Table 4. Results summary for beams with $S_l = 50\%$

V_f : %	P_y : kN	δ_y : mm	P_u : kN	δ_u : mm	P_{max} : kN	$\frac{P_u}{P_{max}}$: %	$\mu = \frac{\delta_u}{\delta_y}$
0 (CB)	192.77	13.76	197.27	17.97	197.27	100	1.31
0	165.58	11.80	165.58	11.80	165.58	100	1.00
1	205.65	13.76	201.16	15.82	205.65	98	1.15
1.5	211.68	13.76	198.80	20.20	211.68	94	1.47
2	217.09	13.76	192.32	27.03	220.75	87	1.96
2.5	222.30	13.76	194.82	24.50	229.20	85	1.78

Table 5. Results summary for beams with $S_l = 100\%$

V_f : %	P_y : kN	δ_y : mm	P_u : kN	δ_u : mm	P_{max} : kN	$\frac{P_u}{P_{max}}$: %	$\mu = \frac{\delta_u}{\delta_y}$
0 (CB)	192.77	13.76	197.27	17.97	197.27	100	1.31
0	122.74	8.20	122.74	8.20	122.74	100	1.00
1	205.44	13.75	205.44	13.75	205.44	100	1.00
1.5	211.49	13.75	200.91	15.81	211.49	95	1.15
2	216.90	13.75	203.71	20.18	220.61	92	1.47
2.5	222.18	13.75	194.78	24.30	229.15	85	1.77

Table 6. Results summary for beams with no stirrups (NS)

$V_f = 0\%$ to $V_f = 2.5\%$) provides an illustration of cracking patterns. It also helps to depict the change in the mode of failure (from a brittle one to a more ductile one). This demonstrates the effectiveness of steel fibres in bridging and controlling cracks.

In the beams without fibres, see Figures 7a(i), 7b(i), 7c(i), 7d(i), the concentration of principal strain vectors was high, indicating a crack pattern that is diagonal and covers the whole of the beam. The diagonal pattern in the beams without fibres deteriorated as the stirrup spacing was increased. The diagonal pattern is characteristic of a shear (and brittle) mode of failure. The addition of fibres, on the other hand, led to a change in crack patterns which became more concentrated in limited

regions near the beam mid-span, which indicates a flexural (and ductile) failure mode. It is interesting to note that for beams with no stirrups (Figure 7(d)), the addition of fibres by up to $V_f = 1\%$ did not seem to alter the failure mode to the desired ductile one. This highlights the severity of the reduction in shear reinforcement when the stirrups were removed completely, which required higher amounts of fibre (i.e. $V_f \geq 1.5\%$) in order to improve the crack pattern and hence the failure mode. These findings were confirmed by comparing the FEA predictions to design code estimates as discussed in Section 4.6. Thus it can be concluded that steel fibres have the potential to compensate for a reduction in conventional transverse shear reinforcement.

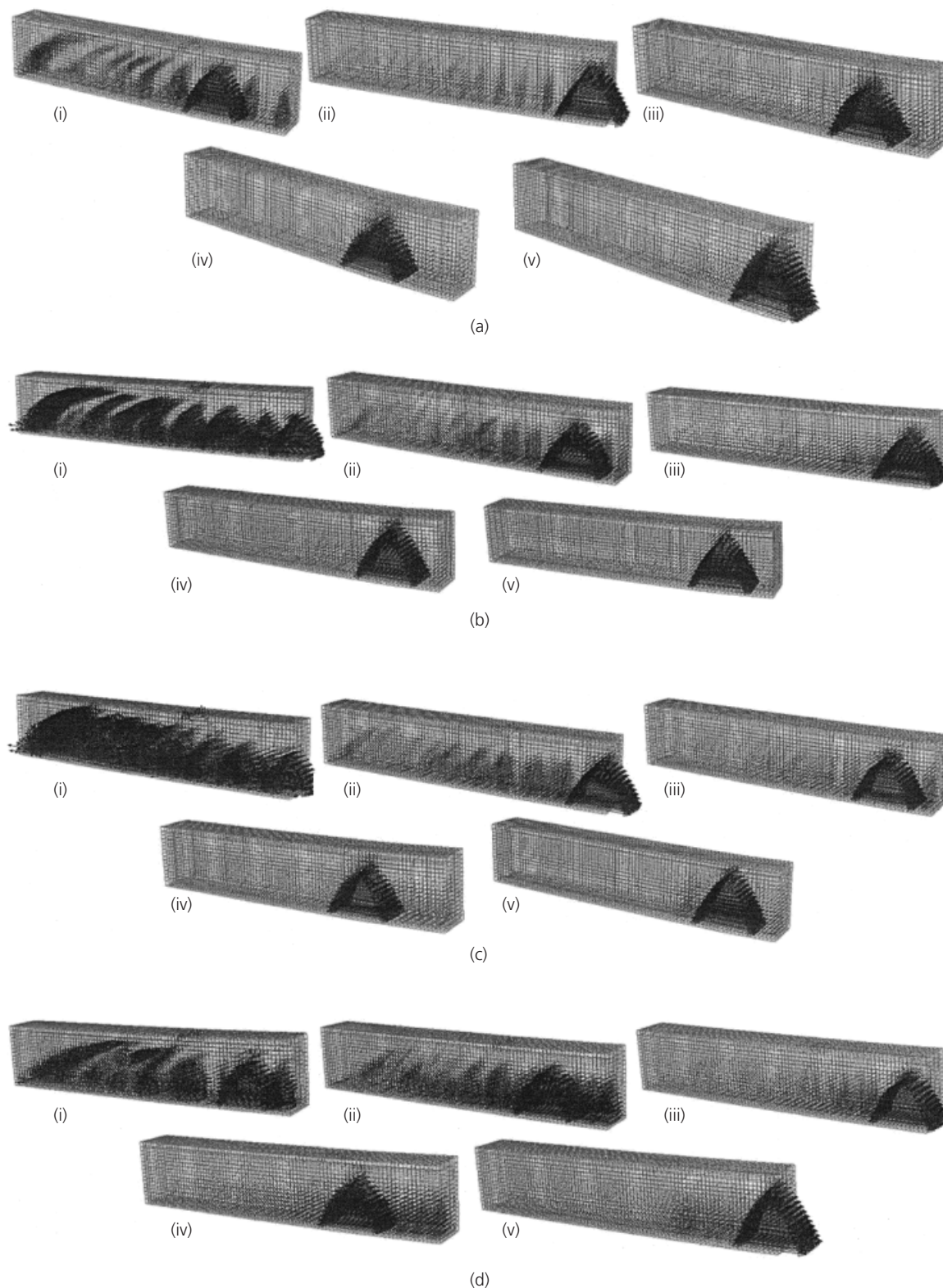


Figure 7. Principal strain vectors for beams with (i) $V_f = 0\%$, (ii) $V_f = 1\%$, (iii) $V_f = 1.5\%$, (iv) $V_f = 2\%$ and (v) $V_f = 2.5\%$; and (a) $SI = 0\%$, (b) $SI = 50\%$, (c) $SI = 100\%$ and (d) no stirrups (NS)

4.5 Comparative study with control specimen using non-dimensional ratios

This section discusses the overall comparison made between the beams analysed with various fibre dosages and increased stirrup spacing and the control beam specimen (i.e. the one with no fibres and no reduction in conventional shear reinforcement).

4.5.1 Strength ratio

The ratios between the maximum load (P_{max}) and yield load (P_y) for each beam and that in the control beam specimen (i.e. $P_{max,0}$ and $P_{y,0}$) are given in Figures 8(a) and 8(b), respectively. Similar patterns were observed from these two figures. Beams without fibres (i.e. $V_f = 0\%$) showed a decrease in both maximum and yield ratios as the stirrup spacing was increased. On the hand, the addition of steel fibres improved both ratios consistently. The increase in both $P_{max}/P_{max,0}$ and $P_y/P_{y,0}$ ratios was by up to ~15%. Adding fibres at $V_f = 1\%$ seemed to restore the strength

level of the control specimen, with more fibres enhancing the strength further.

4.5.2 Ductility ratio

Figure 8(c) presents the results for the ratio between ductility ratio for each beam and that of the control beam specimen plotted against fibre volume fraction. There was a substantial increase in the ductility ratio especially for beams without an increase in stirrups spacing (i.e. $SI = 0\%$) by up to 61% at $V_f = 2\%$. As the spacing between stirrups was increased, the ductility ratio decreased.

It can be concluded that ductility is enhanced as more fibres are added. Interestingly, however, a threshold seems to exist beyond which adding more fibres leads to less rather than more ductility. This can be explained by noting that as the fibre content is increased, the beam becomes stiffer and deflects less (this is largely attributable to the fibres' role in bridging cracks and

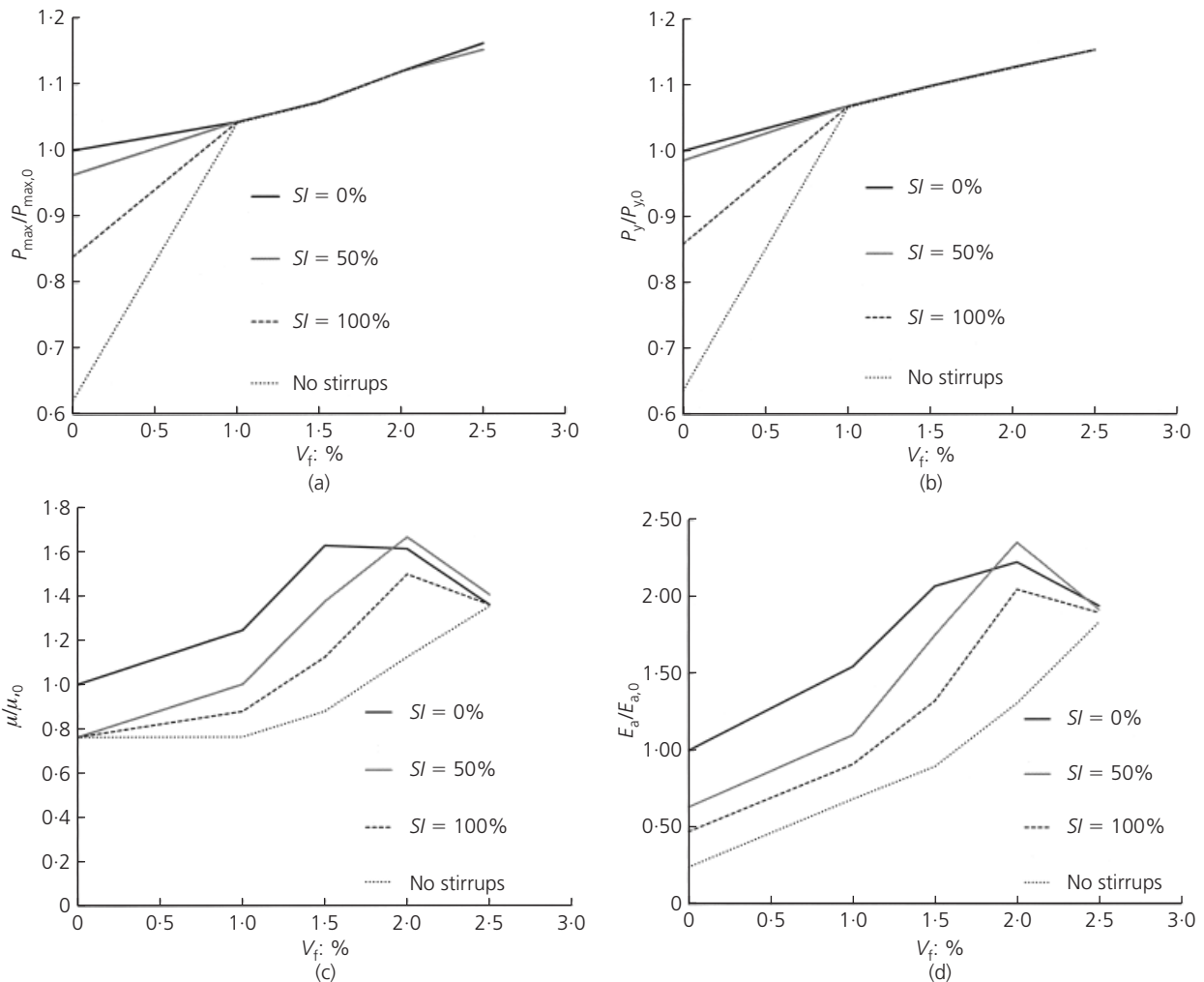


Figure 8. Ratio between key parameters and their corresponding values in the control specimen (i.e. $SI = 0\%$, $V_f = 0\%$) against fibre volume fraction: (a) maximum load, (b) yield load, (c) ductility ratio and (d) energy absorption

limiting their opening). This is similar to the ‘over-reinforced’ behaviour associated with RC design where too much reinforcement leads to a reduction – rather than an increase – in ductility. The optimum fibre contents (i.e. thresholds) were found to be $V_f = 1.5\%$, 2% , 2% and 2.5% for the beams with $SI = 0\%$, 50% , 100% and no stirrups, respectively. The minimum fibre volume fraction required to produce ductility ratios comparable to that associated with the control specimen was found to be $V_f = 1\%$, 1.5% and 2% for the beams with $SI = 50\%$, 100% and no stirrups, respectively. This shows that when the stirrups spacing was increased, a higher amount of fibres was required to retain the same ductility provision. It is important to note that even for the extreme case when all stirrups were completely removed from the beam, the addition of steel fibres still helped restore adequate ductility levels (albeit at a higher fibre content of $V_f = 2\%$ as stated above, highlighting the severity of conventional shear reinforcement reduction).

4.5.3 Energy absorption

Energy absorption is one of the key indicators of structural response as it indicates the structure’s ability to absorb deformations. The ratio between the energy absorption capacity of each beam analysed (E_a) to that of the control specimen ($E_{a,0}$) beams is presented in Figure 8(d). The results confirm the ductility patterns observed in the preceding section. There was a gradual

increase in the energy absorption ratio as the amount of steel fibres was raised up to a certain threshold beyond which energy absorption decreased (this was found to be at $V_f = 2\%$ for all beams except for the one without stirrups). The enhancement in energy absorption was more than double the levels associated with the control specimen, which is a significant improvement.

4.6 Comparison between FEA-based predictions and design calculations

This section discusses the comparison between the FEA results and those calculated according to BS EN 1992-1-1 (BSI, 2004) for conventional RC sections (i.e. without fibres) and Concrete Society TR63 (Concrete Society, 2007) for SFRC beams. The shear (V_{rd}) and bending moment (M_{rd}) capacities were calculated first and then the loads corresponding to shear (P_{SC}) and bending (P_{BMC}) modes of failure were determined. The minimum of these two loads was then used to determine the strength based on current design guidelines ($P_{max,DES}$) and predict the mode of failure. A comparison between the FEA-based load-carrying capacity ($P_{max,FEA}$) and its analytical counterpart ($P_{max,DES}$) was also carried out. Thus, conclusions can be made on the numerical predictions in the light of BS EN 1992-1-1 and Concrete Society TR63 (Concrete Society, 2007) design-based calculations. The results are presented in Tables 7–10. For convenience, the critical values owing to design guidelines are highlighted in bold.

SI = 0		Current design guidelines (DES)				FEA	Comparison
V_f : %	V_{rd} : kN	P_{SC} : kN	M_{rd} : kNm	P_{BMC} : kN	Failure mode	P_{max} : kN	$\frac{P_{max,FEA}}{P_{max,DES}}$
0	105.02	105.02	70.40	113.56	Shear	197.27	1.88
1	123.37	123.37	73.24	118.13	Bending	205.76	1.74
1.5	133.00	133.00	74.59	120.30	Bending	211.69	1.76
2	142.63	142.63	75.89	122.40	Bending	220.74	1.80
2.5	152.26	152.26	77.14	124.42	bending	229.21	1.84

Table 7. Strength predictions based on FEA and current design guidelines for beams with $SI = 0\%$

SI = 50%		Current design guidelines (DES)				FEA	Comparison
V_f : %	V_{rd} : kN	P_{SC} : kN	M_{rd} : kNm	P_{BMC} : kN	Failure mode	P_{max} : kN	$\frac{P_{max,FEA}}{P_{max,DES}}$
0	88.95	88.95	70.40	113.56	Shear	189.94	2.14
1	107.30	107.30	73.24	118.13	Shear	205.77	1.92
1.5	116.93	116.93	74.59	120.30	Shear	211.59	1.81
2	126.56	126.56	75.89	122.40	Bending	220.73	1.80
2.5	136.18	136.18	77.14	124.42	Bending	227.23	1.83

Table 8. Strength predictions based on FEA and current design guidelines for beams with $SI = 50\%$

SI = 100%		Current design guidelines (DES)				FEA	Comparison
V_f : %	V_{rd} : kN	P_{SC} : kN	M_{rd} : kNm	P_{BMC} : kN	Failure mode	P_{max} : kN	$\frac{P_{max,FEA}}{P_{max,DES}}$
0	80.29	80.29	70.40	113.56	Shear	165.58	2.06
1	98.64	98.64	73.24	118.13	Shear	205.65	2.08
1.5	108.27	108.27	74.59	120.30	Shear	211.68	1.96
2	117.90	117.90	75.89	122.40	Shear	220.75	1.87
2.5	127.53	127.53	77.14	124.42	Bending	229.20	1.84

Table 9. Strength predictions based on FEA and current design guidelines for beams with $SI = 100\%$

NS		Current design guidelines (DES)				FEA	Comparison
V_f : %	V_{rd} : kN	P_{SC} : kN	M_{rd} : kNm	P_{BMC} : kN	Failure mode	P_{max} : kN	$\frac{P_{max,FEA}}{P_{max,DES}}$
0	55.57	55.57	70.40	113.56	Shear	122.74	2.21
1	73.92	73.92	73.24	118.13	Shear	205.44	2.78
1.5	83.55	83.55	74.59	120.30	Shear	211.49	2.53
2	93.18	93.18	75.89	122.40	Shear	220.61	2.37
2.5	102.81	102.81	77.14	124.42	Shear	229.15	2.23

Table 10. Strength predictions based on FEA and current design guidelines for beams with no stirrups

The values of the shear capacity V_{rd} for SFRC sections with shear links were calculated using the method recommended by Rilem Technical Committees (2003), which simply comprises the contribution of the fibres determined from the Rilem guide and the contributions of concrete (i.e. aggregate interlock, dowel action and concrete in the compression zone) and shear links determined from BS EN 1992-1-1. Thus, V_{rd} can be defined as follows

$$1. \quad V_{rd} = V_{rd,c} + V_{fd} + V_{wd}$$

where $V_{rd,c}$, V_{fd} and V_{wd} are the contributions of concrete, fibres and shear links, respectively. The method was updated in Concrete Society TR63 (Concrete Society, 2007) to conform to the latest recommendations of BS EN 1992-1-1, leading to the following expression for V_{rd}

$$2. \quad V_{rd} = \left[\left(\frac{0.18}{\gamma_c} \right) k (100 \rho_l f_{ck})^{1/3} + v_{fd} \right] bd + V_{wd}$$

where γ_c is the material partial safety factor for concrete taken as

1.5, $k = 1 + (200/d)^{1/2} \leq 2$ (where d is the effective depth of the beam in mm) and $\rho_l = A_{sl}/bd \leq 0.02$ (where A_{sl} is the area of the tensile flexural reinforcement, b is the width of the beam cross-section, v_{fd} is the shear strength contribution due to fibres and V_{wd} is the contribution of shear links). The value of v_{fd} can be determined from the following equation proposed by Rilem

$$3. \quad v_{fd} = 0.7 k_f k \tau_{fd}$$

where k_f is a factor taking into account contribution of flanges in a T-section (which was taken as 1.0 for the present case of a rectangular cross-section) and τ_{fd} is the design value of the increase in shear strength owing to fibres. The value of V_{wd} can be determined from BS EN 1992-1-1 using the following equation for the present case of vertical shear links

$$4. \quad V_{wd} = 0.9 d (A_{sw}/S) f_{ywd}$$

where A_{sw} is the cross-sectional area of shear links, S is the spacing between the shear links and f_{ywd} is their yield strength. The resistance of the members without shear reinforcement was

based on Equation 2, but with the term V_{wd} being omitted. A strut capacity check was also carried out as recommended in BS EN 1992-1-1. The bending moment capacity of SFRC sections was also determined by adjusting the recommendations of BS EN 1992-1-1 to allow for the effect of fibres as proposed in Concrete Society TR63. This was simply achieved by introducing a rectangular tensile stress block (extending from the neutral axis to the bottom of the section) with a strength value f_{td} . Consequently the resultant tensile force was determined and the corresponding moment capacity was added to the moment components calculated based on the concrete stress block in compression and the longitudinal steel in both the tensile and compressive regions of the beam cross-section.

The results obtained show that steel fibres increase the load-carrying capacity of the beams. The FEA-based predictions were consistently higher than those estimated based on current design guidelines. To establish which of the two sets of predictions is closer to the actual structural response, both were compared to existing experimental data (Campione *et al.*, 2006). The findings of this comparative study are presented in Table 11, which shows that the FEA-based results are in extremely good agreement with the experimental data. The only exception is the highly non-linear case of the beam with no stirrups and no fibres (i.e. NS and $V_f = 0\%$) where the numerical predictions are higher than the corresponding experimental values, pointing to the need for further examination of this complex case, which can be challenging to study both numerically and experimentally (and which is not usually encountered in practice as some minimum nominal stirrup amount is invariably provided).

The comparative study shows that for all SFRC beams considered, the FEA-based results show remarkable agreement with the experimental data confirming the validity of the numerical results. Thus, it can be concluded that the FEA provided estimates of load-carrying capacity for SFRC beams which are more economical than those based on current design guidelines (i.e. Concrete Society, 2007). This is largely because the numerical results are based on 3D modelling compared to the code simplified 1D sectional analysis (so effects such as confinement and the triaxial state of stresses are not included in the latter). Further studies are

needed to ascertain the conservatism of current guidelines and to examine the trend in more detail.

In the current study, the conventional RC beams (i.e. without fibres) were initially designed with reduced shear reinforcement in order to induce a shear mode of failure. It is interesting to see that the addition of fibres has led to a change in the failure mode from a brittle one (i.e. shear) to a more ductile one (i.e. bending), which is desired in design. This is true even for the case with severe conventional shear reduction when stirrups were completely removed as the brittle failure mode was reversed to a ductile one with fibres added at $V_f = 2\% \sim 2.5\%$. For the rest of the beams the addition of fibres, even at 1%, changed the mode failure of the beam from shear to bending. It can be concluded that steel fibres increase the load-carrying capacity of the beams and ensure a more ductile structural response (thus avoiding a brittle shear mode of failure).

5. Conclusion

Fibres are utilised in order to enhance the properties of an inherently brittle and crack-prone cement-based matrix. Parametric studies on SFRC beams under monotonic loading were carried out by means of NLFEA. The latter were initially calibrated and verified against existing experimental data of Campione *et al.* (2006). The investigation is focused on simply supported beams, which were designed with reduced shear reinforcement in order to incorporate a shear mode of failure. The spacing between shear stirrups was increased (with the extreme case of beams without transverse stirrups being considered as well), while fibres were added to examine their potential as a substitute for the loss in conventional shear reinforcement.

Based on the findings of the present investigation, it can be concluded that the addition of steel fibres consistently enhances the load-carrying capacity. The strength increase was by up to $\sim 15\%$ compared to the control beam specimen (i.e. the one with no increase in stirrups spacing and no fibres). Furthermore, fibres were found to increase stiffness, leading to reduced deflections. This shows that there are clear benefits of adding fibres at both the serviceability and ultimate limit states, which are important design considerations. The addition of steel fibres also led to a reduction in crack formation and propagation. It has also

S_l : %	V_f : %	$P_{max,FEA}$: kN	$P_{max,DES}$: kN	$P_{max,EXP}$: kN	$\frac{P_{max,FEA}}{P_{max,DES}}$	$\frac{P_{max,FEA}}{P_{max,EXP}}$	$\frac{P_{max,DES}}{P_{max,EXP}}$
50	1	205.77	107.30	205.00	1.92	1.00	0.52
50	2	220.73	122.40	242.90	1.80	0.91	0.50
NS	0	122.74	55.57	86.10	2.21	1.43	0.65
NS	1	205.44	73.92	191.80	2.78	1.07	0.39
NS	2	220.61	93.18	209.14	2.37	1.06	0.45

Table 11. A comparative study between load-carrying capacity based on FEA, current design guidelines and existing experimental results

improved the structural response by altering the failure mode from a brittle shear mode to a flexural ductile one, which is desired in design.

As the fibre amount was increased, ductility also improved. Interestingly, it was found that the increase in ductility seems to reduce if excessive amounts of fibres are provided. This suggests that there is an optimum amount of fibres that can be added to enhance ductility. This is similar to the situation experienced in RC design when reinforcement is increased beyond a certain threshold (i.e. 'balanced section'), which leads to increase in strength but reduction in ductility. A similar pattern was observed for energy absorption which, alongside ductility, is an important indicator of structural performance. The increase in ductility is accompanied by a softening load–deflection response. However, the residual strength was found to be sufficiently high (i.e. >85%) in all cases studied, suggesting the softening is not significant from a practical design viewpoint. The optimum fibre contents were found to be $V_f = 1.5\%$, 2%, 2% and 2.5% for the beams with $SI = 0\%$, 50%, 100% and no stirrups, respectively. It is important to note that even for the extreme case when all stirrups were completely removed from the beam (i.e. no stirrups), the addition of fibres still resulted in restoring adequate ductility levels (albeit at a higher fibre content of $V_f = 2\%$ owing to the severity of conventional shear reinforcement removal).

Flexural and shear capacities were also calculated using analytical expressions given in BS EN 1992-1-1 (BSI, 2004) for conventional RC sections (i.e. without fibres) and Concrete Society TR63 (Concrete Society, 2007) for SFRC beams. These were compared with the FEA-based strength values. The numerical and analytical data sets were also compared to existing experimental results which confirmed the validity of the FEA-based predictions. The numerical results were found to be more economical than the corresponding estimates based on current design guidelines. The study has also confirmed the potential for fibres to compensate for a reduction in conventional shear reinforcement.

In summary, it can be concluded that steel fibres increase load-carrying capacity and limit crack propagation. They also enhance ductility and energy absorption (with associated optimum/threshold fibre contents determined). A comparison between the SFRC beams with and without shear links demonstrates that fibres have the potential to compensate for a reduction in shear links. This can be useful in situations where the amount of shear reinforcement required can lead to congestion of the links and can also simplify complex construction arrangements.

REFERENCES

Abaqus (2007) *Version 6.7 Documentation*. See <http://www.simulia.com/services/training/V67-Introduction-DEMO/AbaqusV67Intro.htm> (accessed 12/11/2013).

- Abbas AA, Syed Mohsin SM and Cotsovos DM (2010a) Numerical modelling of fibre-reinforced concrete. In *Proceedings of the International Conference on Computing in Civil and Building Engineering ICCBE 2010, Nottingham, UK* (Tizani W (ed.)). University of Nottingham Press, Nottingham, UK, p. 473, Paper 237.
- Abbas AA, Syed Mohsin SM and Cotsovos DM (2010b) A comparative study on modelling approaches for fibre-reinforced concrete. *Proceedings of the 9th HSTAM International Congress on Mechanics, Limassol, Cyprus*.
- Barros JA and Figueiras JA (1999) Flexural behavior of SFRC: Testing and modelling. *Journal of Materials in Civil Engineering, ASCE* **11(4)**: 331–339.
- Barros JA and Figueiras JA (2001) Model for the analysis of steel fibre reinforced concrete slabs on grade. *Computers and Structures* **79(1)**: 97–106.
- Bencardino F, Rizzuti L, Spadea G and Ramnath N (2008) Stress-strain behavior of steel fiber-reinforced concrete in compression. *Journal of Materials in Civil Engineering, ASCE* **20(3)**: 255–262.
- Bresler G and Scordelis A (1963) Shear strength of reinforced concrete beams. *ACI Journal* **60(1)**: 51–74.
- BSI (2004) BS EN 1992-1-1:2004. Eurocode 2: Design of concrete structures – Part 1-1: General rules and rules for buildings. BSI, London, UK.
- Campione G, La Mendola L and Papia M (2006) Shear strength of steel fibre reinforced concrete beams with stirrups. *Structural Engineering and Mechanics* **24(1)**: 107–136.
- Cho SH and Kim YI (2003) Effects of steel fibres on short beams loaded in shear. *ACI Structural Journal* **100(6)**: 765–774.
- Concrete Society (2007) *Guidance for the Design of Steel-Fibre-Reinforced Concrete*. Concrete Society, Camberley, UK, Technical Report No. 63.
- Hughes G and Spiers D (1982) *An Investigation on the Beam Impact Problem*. Cement and Concrete Association, Slough, UK, Technical Report 546.
- Lok TS and Pei JS (1996) Flexural behavior of steel fiber-reinforced concrete. *Journal of Materials in Civil Engineering, ASCE* **10(2)**: 86–97.
- Lok TS and Xiao JR (1999) Flexural strength assessment of steel fiber-reinforced concrete. *Journal of Materials in Civil Engineering, ASCE* **11(3)**: 188–196.
- Rilem Technical Committees (2000) Rilem TC 162-TDF: Test and design methods for steel fibre-reinforced concrete, recommendation: σ – ϵ design method. *Materials and Structures, Rilem* **33(2)**: 75–81.
- Rilem Technical Committees (2003) Rilem TC 162-TDF: Test and design methods for steel fibre-reinforced concrete, final recommendation: σ – ϵ design method. *Materials and Structures, Rilem* **36(8)**: 560–567.
- Sharma AK (1986) Shear strength of steel fibre reinforced concrete beams. *ACI Journal* **83(4)**: 624–628.
- Syed Mohsin SM (2012) *Behaviour of Fibre-reinforced Concrete Structures under Seismic Loading*. PhD thesis, Imperial College London, London, UK.

Tlemat H, Pilakoutas K and Neocleous K (2006) Modelling of SFRC using inverse finite element analysis. *Materials and Structures, Rilem* **39(2)**: 221–233.

Zheng Y, Robinson D, Taylor S and Cleland D (2012) Non-linear finite-element analysis of punching capacities of steel–

concrete bridge deck slabs. *Proceedings of the Institution of Civil Engineers – Structures and Buildings* **165(5)**: 255–259.

Zienkiewicz OC and Taylor RL (2005) *Vol. 2: The Finite Element Method for Solid and Structural Mechanics*, 6th edn. Butterworth-Heinemann, Oxford, UK.

WHAT DO YOU THINK?

To discuss this paper, please email up to 500 words to the editor at journals@ice.org.uk. Your contribution will be forwarded to the author(s) for a reply and, if considered appropriate by the editorial panel, will be published as a discussion in a future issue of the journal.

Proceedings journals rely entirely on contributions sent in by civil engineering professionals, academics and students. Papers should be 2000–5000 words long (briefing papers should be 1000–2000 words long), with adequate illustrations and references. You can submit your paper online via www.icevirtuallibrary.com/content/journals, where you will also find detailed author guidelines.